

# Ignition of *n*-Hexane–Air by Moving Hot Particles: Effect of Particle Diameter

Stephanie Coronel    Josue Melguizo-Gavilanes    Joseph E. Shepherd

Graduate Aeronautical Laboratories, California Institute of Technology

9th US National Combustion Meeting

Cincinnati, Ohio  
May 17 - 20, 2015



# Hot Particle Ignition Sources

- Lightning attaches to the top of the fastener and causes damage to the resin and fibers on the backface of the composite laminate
- The breakup of the composite is due to its poor electrical conductivity that leads to resistive heating



P. Feraboli, M. Miller. Composites Part A: Applied Science and Manufacturing, Volume 40, Issues 6-7, July 2009, Pages 954-967



Ignition at edge of carbon fiber composite structure, Boeing

# Hot Particle Ignition Sources

- Lightning attaches to the top of the fastener and causes damage to the resin and fibers on the backface of the composite laminate
- The breakup of the composite is due to its poor electrical conductivity that leads to resistive heating



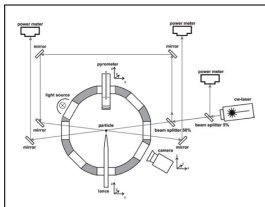
P. Feraboli, M. Miller. Composites Part A: Applied Science and Manufacturing, Volume 40, Issues 6-7, July 2009, Pages 954-967



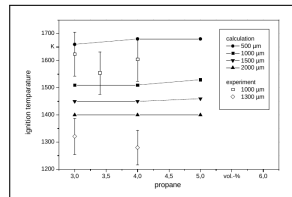
Ignition at edge of carbon fiber composite structure, Boeing

# Stationary Hot Particle Ignition

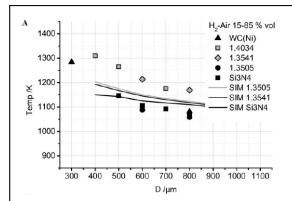
- H. Bothe et al. In *Explosion Safety in Hazardous Areas*, 1999. International Conference on (Conf. Publ. No. 469), pages 44–49, 1999
- T. H. Dubaniewicz et al. (2000, 2003)
- T. H. Dubaniewicz. *Journal of Laser Applications*, 18 (2006) 312–319



- M. Beyer and D. Markus. *Sci. Tech. Energetic Materials*, (2012)
- D. Roth et al. *Combustion Science and Technology*, 186 (2014) 1606–1617

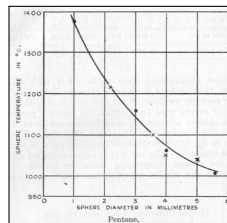
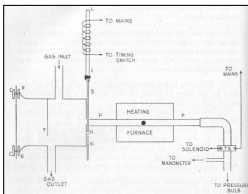


M. Beyer and D. Markus (2012)



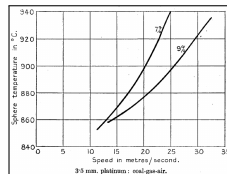
Roth et al. (2014)

# Moving Hot Particle Ignition



R. Silver (1937)

- R. S. Silver. The London, Edinburgh, and Dublin Philosophical Magazine and Journal of Science, 23 (1937) 633-657
- S. Patterson. The London, Edinburgh, and Dublin Philosophical Magazine and Journal of Science, 28 (1939) 1-22
- S. Patterson. The London, Edinburgh, and Dublin Philosophical Magazine and Journal of Science, 30 (1940) 437-457



S. Patterson (1940)

# Current study

Material	$d$ (mm)	$V_p$ (m/s)	$T_{sphere}$ (K)
alumina	6.0, 3.5, 1.8	2.3 – 2.4	800 – 1200

Mixture	$T_0$ (K)	$P_0$ (kPa)	$\Phi$
<i>n</i> -hexane–air	300	100	0.7 – 2.2

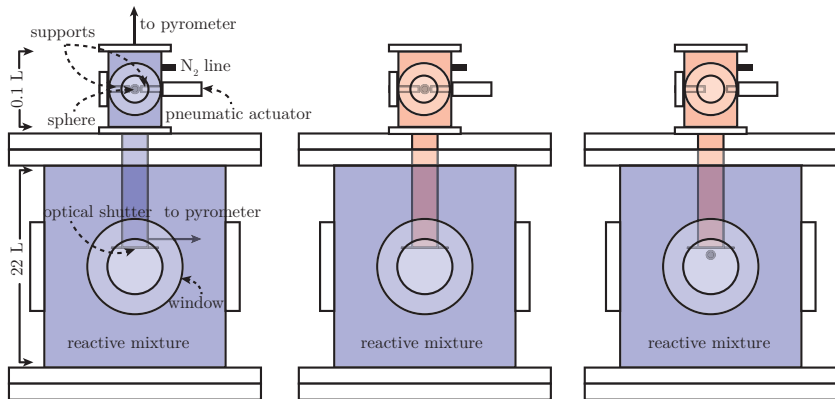
# Current study

Material	$d$ (mm)	$V_p$ (m/s)	$T_{sphere}$ (K)
alumina	6.0, 3.5, 1.8	2.3 – 2.4	800 – 1200

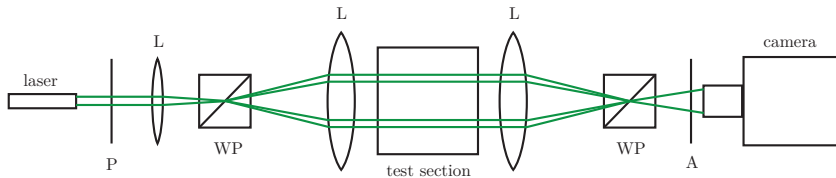
Mixture	$T_0$ (K)	$P_0$ (kPa)	$\Phi$
<i>n</i> -hexane–air	300	100	0.7 – 2.2

$$\Phi = 0.9$$

# Experimental Setup: Combustion Vessel

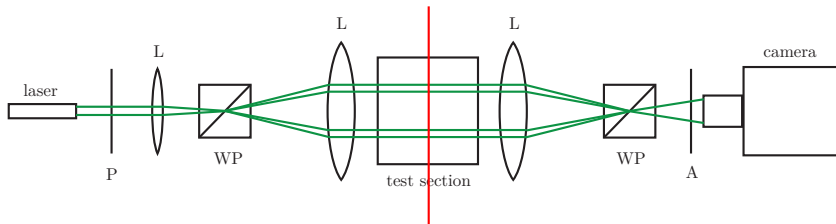


# Optical Diagnostics: Shearing Interferometer



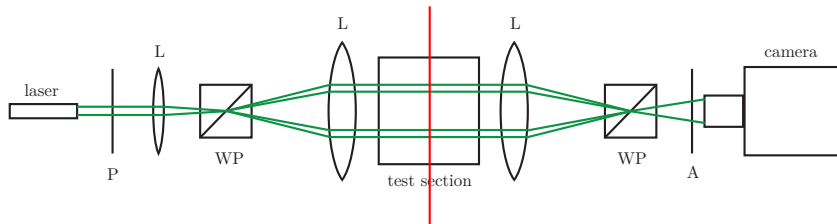
P: polarizer, L: lens, WP: Wollaston prism, A: Analyzer

# Optical Diagnostics: Shearing Interferometer

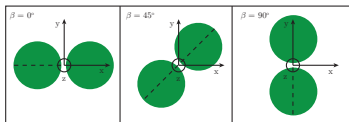


P: polarizer, L: lens, WP: Wollaston prism, A: Analyzer

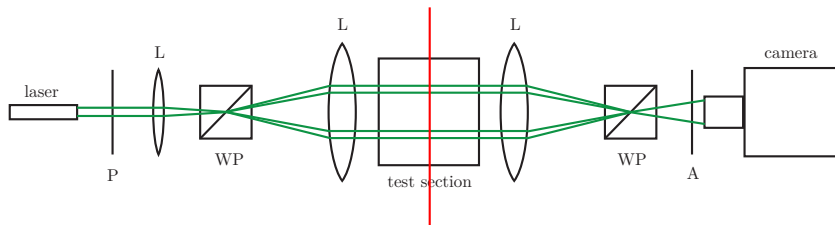
# Optical Diagnostics: Shearing Interferometer



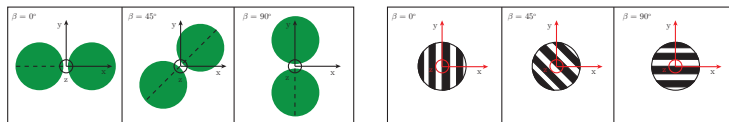
P: polarizer, L: lens, WP: Wollaston prism, A: Analyzer



# Optical Diagnostics: Shearing Interferometer



P: polarizer, L: lens, WP: Wollaston prism, A: Analyzer



Finite fringe configurations

# Simulation Setup

## ■ Grid

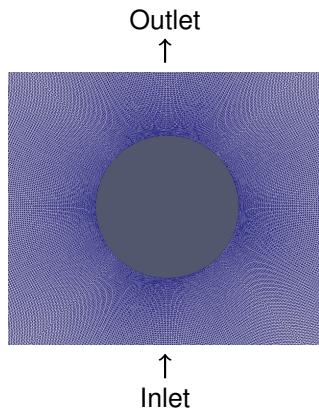
- 2D axisymmetric
- Square of size  $20d$
- 300,000 cells
- Sphere vicinity ( $40 \mu\text{m}$  cell size)

## ■ Boundary conditions

- $T_{\text{sphere}} = \text{constant}$
- $T_{\text{wall}} = 300 \text{ K}$
- Inert surface
- Neumann boundary condition for species

## ■ Initial conditions

- $P_0 = 100 \text{ kPa}$ ,  $T_0 = 300 \text{ K}$  and  $\Phi = 0.9$
- Flow  $\text{N}_2$  at  $t = 0 - 250 \text{ ms}$  and  $\mathbf{u} = (0, gt, 0)$
- One-step  $n$ -hexane<sup>1</sup>-air ( $R \rightarrow P$ ) at  $t > 250 \text{ ms}$



- OpenFOAM: Variable-density reactive Navier-Stokes equations

# Simulation Setup

## Grid

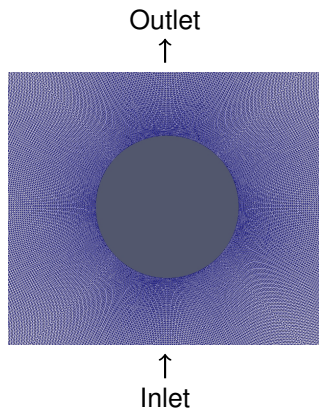
- 2D axisymmetric
- Square of size  $20d$
- 300,000 cells
- Sphere vicinity ( $40 \mu\text{m}$  cell size)

## Boundary conditions

- $T_{\text{sphere}} = \text{constant}$
- $T_{\text{wall}} = 300 \text{ K}$
- Inert surface
- Neumann boundary condition for species

## Initial conditions

- $P_0 = 100 \text{ kPa}$ ,  $T_0 = 300 \text{ K}$  and  $\Phi = 0.9$
- Flow  $\text{N}_2$  at  $t = 0 - 250 \text{ ms}$  and  $\mathbf{u} = (0, gt, 0)$
- One-step  $n$ -hexane<sup>1</sup>-air ( $R \rightarrow P$ ) at  $t > 250 \text{ ms}$



- OpenFOAM: Variable-density reactive Navier-Stokes equations

# Simulation Setup

## ■ Grid

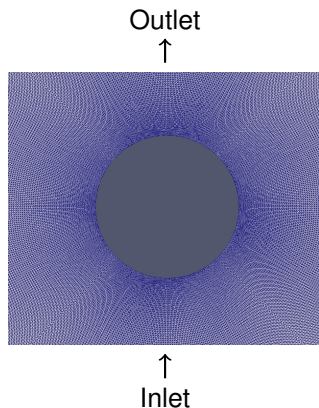
- 2D axisymmetric
- Square of size  $20d$
- 300,000 cells
- Sphere vicinity ( $40 \mu\text{m}$  cell size)

## ■ Boundary conditions

- $T_{\text{sphere}} = \text{constant}$
- $T_{\text{wall}} = 300 \text{ K}$
- Inert surface
- Neumann boundary condition for species

## ■ Initial conditions

- $P_0 = 100 \text{ kPa}$ ,  $T_0 = 300 \text{ K}$  and  $\Phi = 0.9$
- Flow  $\text{N}_2$  at  $t = 0 - 250 \text{ ms}$  and  $\mathbf{u} = (0, gt, 0)$
- One-step  $n$ -hexane<sup>1</sup>-air ( $R \rightarrow P$ ) at  $t > 250 \text{ ms}$



- OpenFOAM: Variable-density reactive Navier-Stokes equations

<sup>1</sup> H. P. Ramirez et al. (2011). Proceedings of the Combustion Institute, 33

# Simulation Setup

## Grid

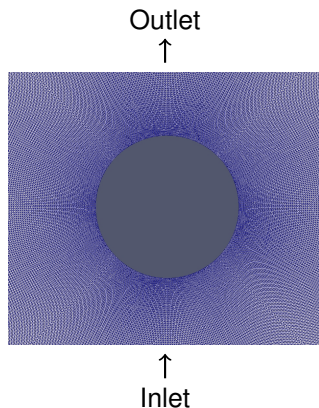
- 2D axisymmetric
- Square of size  $20d$
- 300,000 cells
- Sphere vicinity ( $40 \mu\text{m}$  cell size)

## Boundary conditions

- $T_{\text{sphere}} = \text{constant}$
- $T_{\text{wall}} = 300 \text{ K}$
- Inert surface
- Neumann boundary condition for species

## Initial conditions

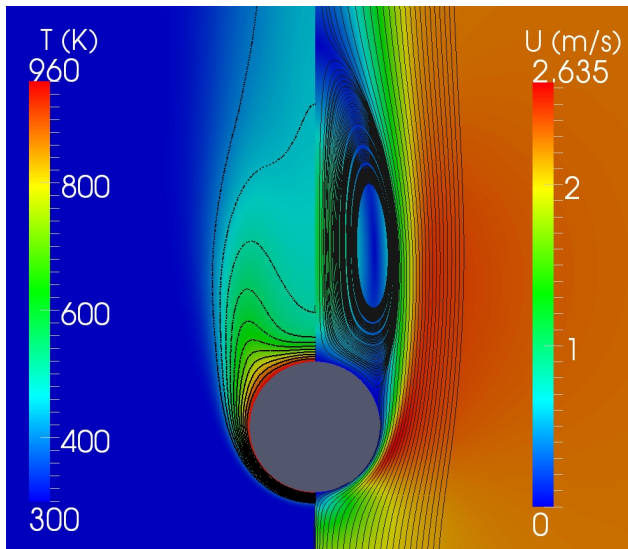
- $P_0 = 100 \text{ kPa}$ ,  $T_0 = 300 \text{ K}$  and  $\Phi = 0.9$
- Flow  $\text{N}_2$  at  $t = 0 - 250 \text{ ms}$  and  $\mathbf{u} = (0, gt, 0)$
- One-step  $n$ -hexane<sup>1</sup>-air ( $R \rightarrow P$ ) at  $t > 250 \text{ ms}$



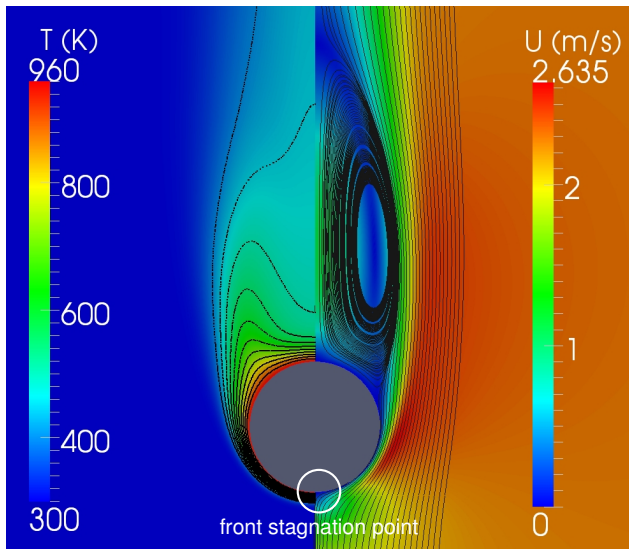
- OpenFOAM: Variable-density reactive Navier-Stokes equations

<sup>1</sup> H. P. Ramirez et al. (2011). Proceedings of the Combustion Institute, 33

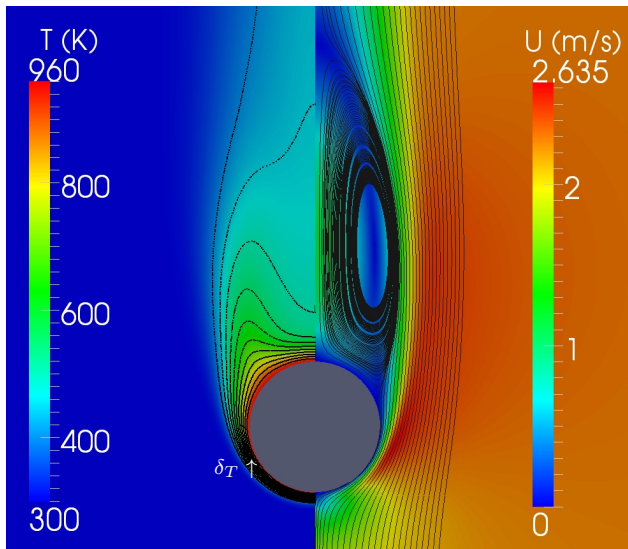
# N<sub>2</sub> Hot Particle Wake (Simulation)



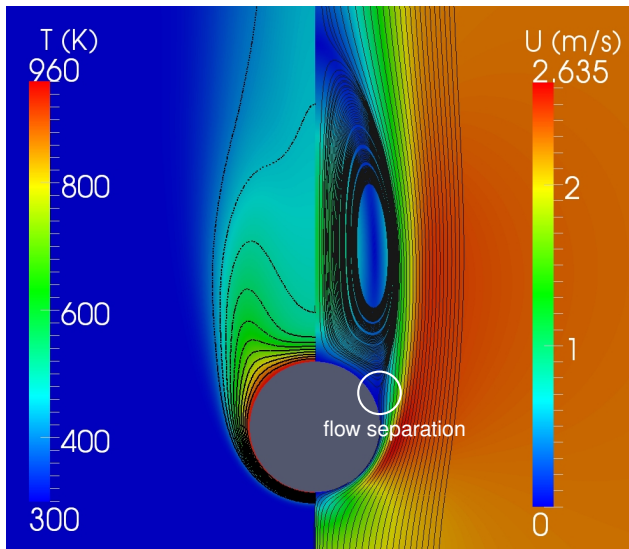
# N<sub>2</sub> Hot Particle Wake (Simulation)



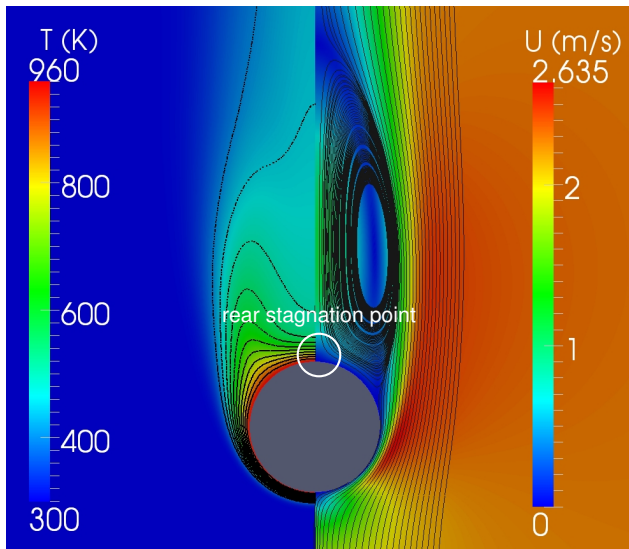
# N<sub>2</sub> Hot Particle Wake (Simulation)



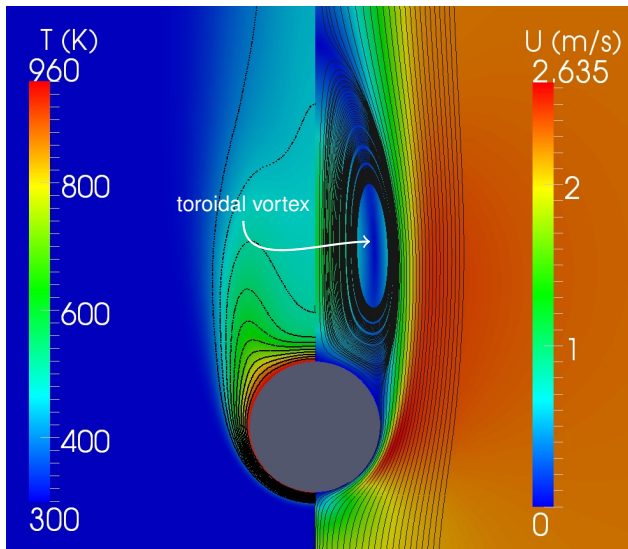
# N<sub>2</sub> Hot Particle Wake (Simulation)



# N<sub>2</sub> Hot Particle Wake (Simulation)

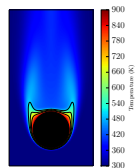
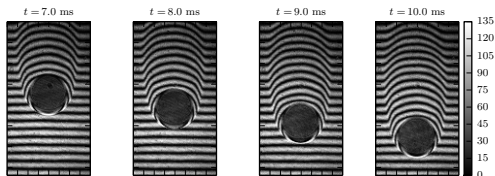


# N<sub>2</sub> Hot Particle Wake (Simulation)

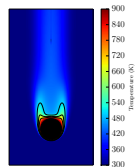
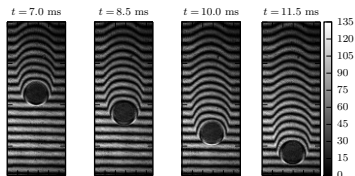


# Unreacted Hot Particle Wake: $\approx 900$ K (Exp. and Sim.)

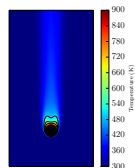
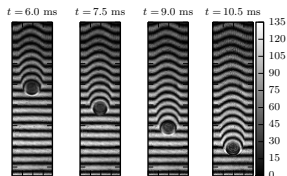
$d = 6.0$  mm



$d = 3.5$  mm

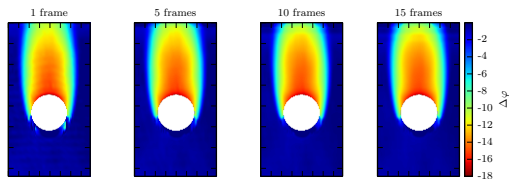


$d = 1.8$  mm



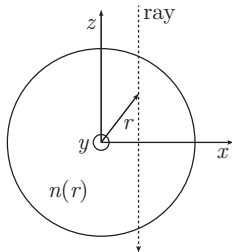
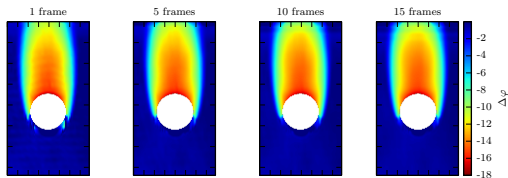
# Unreacted Hot Particle Wake (Experiment)

Time averaged  
unwrapped  
optical phase



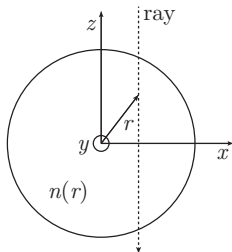
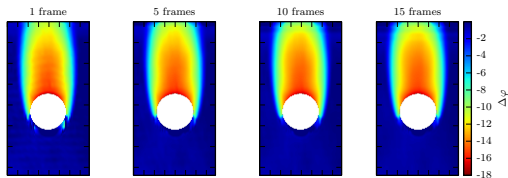
# Unreacted Hot Particle Wake (Experiment)

Time averaged  
unwrapped  
optical phase



# Unreacted Hot Particle Wake (Experiment)

Time averaged  
unwrapped  
optical phase

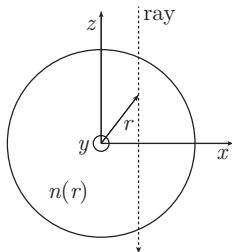
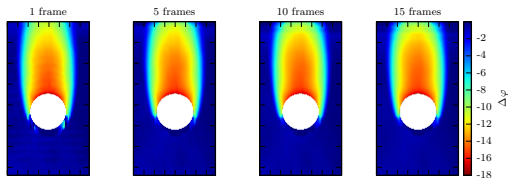


Abel transform

$$F(x) = 2 \int_x^\infty \frac{f(r)r}{(r^2 - x^2)^{1/2}} dr. \quad (1)$$

# Unreacted Hot Particle Wake (Experiment)

Time averaged  
unwrapped  
optical phase



Abel transform

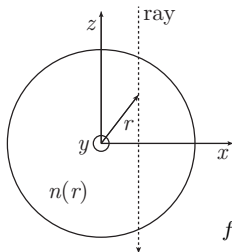
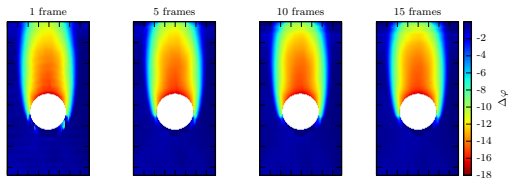
$$F(x) = 2 \int_x^\infty \frac{f(r)r}{(r^2 - x^2)^{1/2}} dr. \quad (1)$$

The inverse Abel transform is given by

$$f(r) = -\frac{1}{\pi} \int_r^\infty \frac{dF}{dx} \frac{dx}{(x^2 - r^2)^{1/2}}, \quad (2)$$

# Unreacted Hot Particle Wake (Experiment)

Time averaged  
unwrapped  
optical phase



Abel transform

$$F(x) = 2 \int_x^\infty \frac{f(r)r}{(r^2 - x^2)^{1/2}} dr. \quad (1)$$

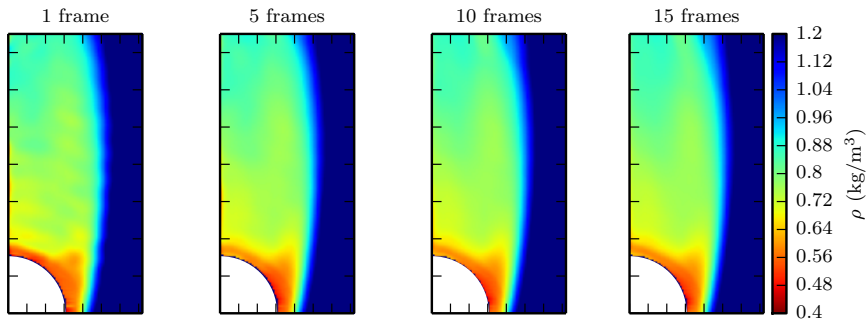
The inverse Abel transform is given by

$$f(r) = -\frac{1}{\pi} \int_r^\infty \frac{dF}{dx} \frac{dx}{(x^2 - r^2)^{1/2}}, \quad (2)$$

$$f(r) = \frac{2\pi}{\lambda} [n(r) - n_o(r)] \quad \text{and} \quad F(x) = \Delta\varphi \quad (3)$$

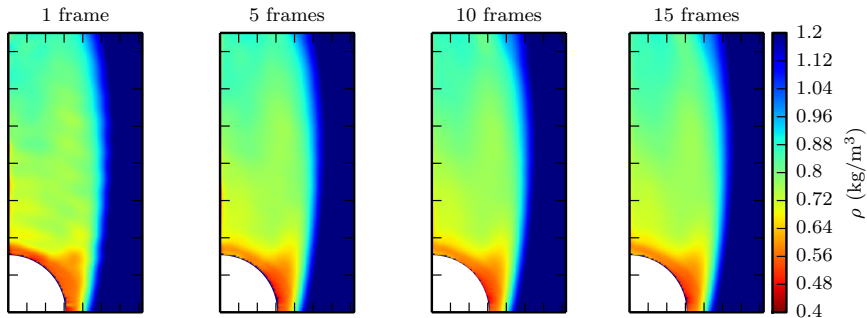
# Unreacted Hot Particle Wake (Experiment)

Gladstone-Dale relation  $n - 1 = K\rho$



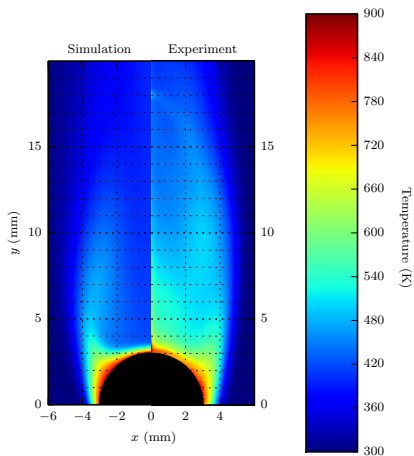
# Unreacted Hot Particle Wake (Experiment)

Gladstone-Dale relation  $n - 1 = K\rho$

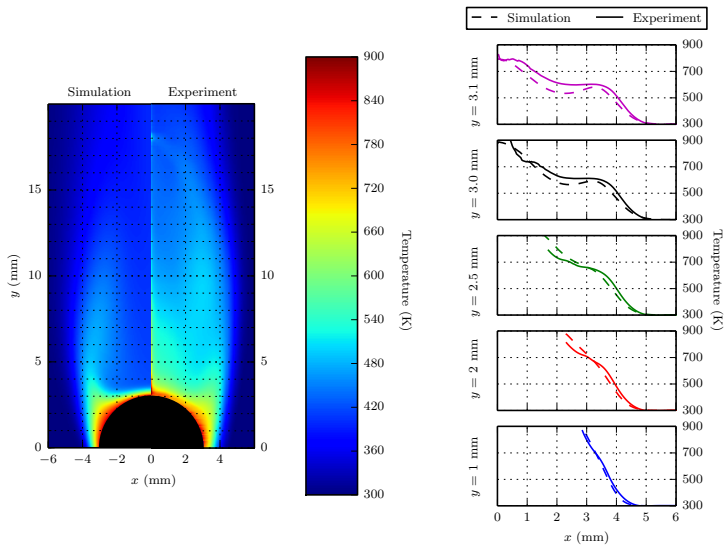


$$P = \rho RT$$

# Unreacted Hot Particle Wake: Validation



# Unreacted Hot Particle Wake: Validation

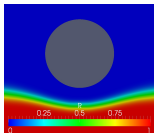


# Ignition (Experiment)

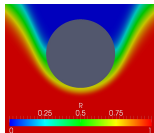
1.8 mm

# Ignition (Simulation)

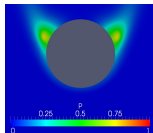
$t = 1.25$  ms



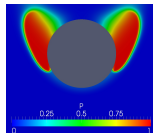
$t = 5.00$  ms



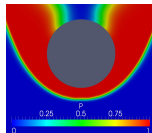
$t = 15.0$  ms



$t = 15.5$  ms

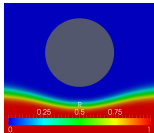


$t = 16.25$  ms

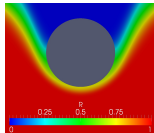


# Ignition (Simulation)

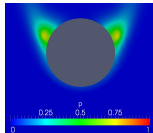
$t = 1.25$  ms



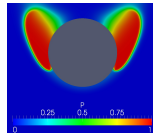
$t = 5.00$  ms



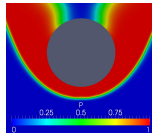
$t = 15.0$  ms



$t = 15.5$  ms



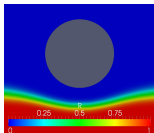
$t = 16.25$  ms



Arrival of  
reactive mixture  
(R)

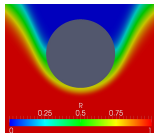
# Ignition (Simulation)

$t = 1.25$  ms



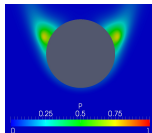
Arrival of  
reactive mixture  
(R)

$t = 5.00$  ms

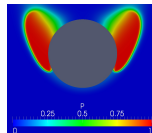


Contact of  
reactive mixture  
(R) with hot  
sphere

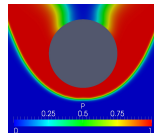
$t = 15.0$  ms



$t = 15.5$  ms

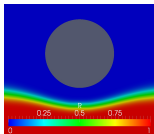


$t = 16.25$  ms



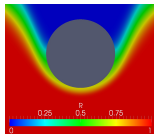
# Ignition (Simulation)

$t = 1.25$  ms



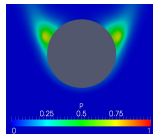
Arrival of  
reactive mixture  
(R)

$t = 5.00$  ms



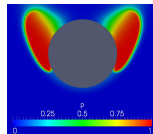
Contact of  
reactive mixture  
(R) with hot  
sphere

$t = 15.0$  ms

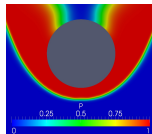


Creation of  
products (P)

$t = 15.5$  ms

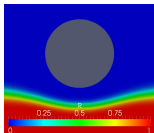


$t = 16.25$  ms



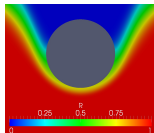
# Ignition (Simulation)

$t = 1.25$  ms



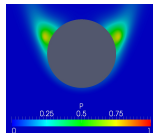
Arrival of  
reactive mixture  
(R)

$t = 5.00$  ms



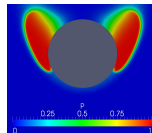
Contact of  
reactive mixture  
(R) with hot  
sphere

$t = 15.0$  ms



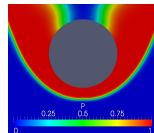
Creation of  
products (P)

$t = 15.5$  ms



Flame  
propagation

$t = 16.25$  ms



Flame  
propagation

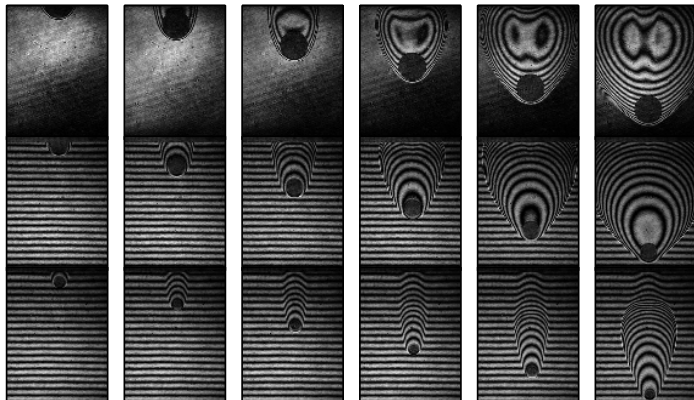
# Flame Propagation (Experiment)

Recall:  $\Phi = 0.9$     Current flame:  $S_b = 2.6$  m/s    Particle speed:  $V_p = 2.3 - 2.4$  m/s

$d = 6.0$  mm

$d = 3.5$  mm

$d = 1.8$  mm



1.5 ms

3.5 ms

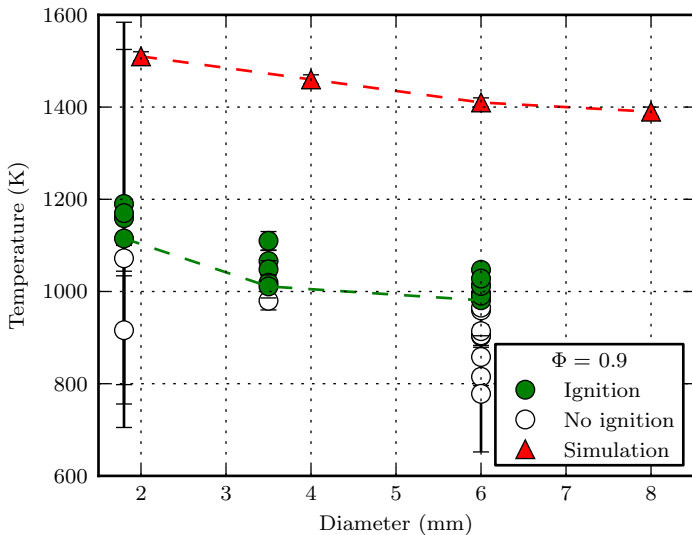
5.5 ms

7.5 ms

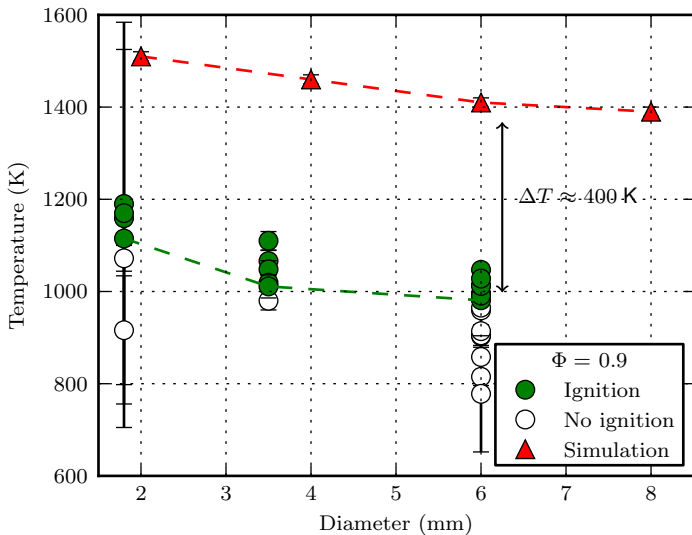
9.5 ms

11.5 ms

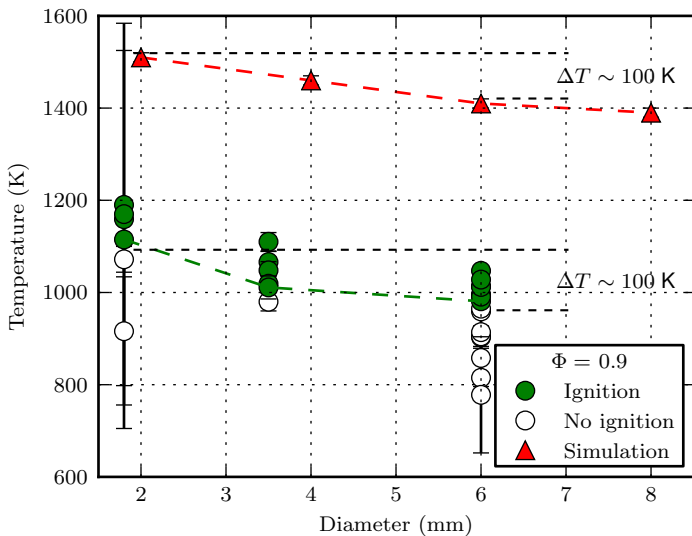
# Ignition Thresholds (Exp. and Sim.)



# Ignition Thresholds (Exp. and Sim.)

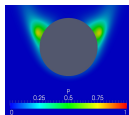


# Ignition Thresholds (Exp. and Sim.)



# Conclusions

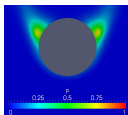
- Simulation predicts ignition to occur in the flow separation region



- The ignition threshold was found to be  $981 \pm 10$  K,  $1010 \pm 25$  K, and  $1159 \pm 10$  K, for sphere diameters of 6.0 mm, 3.5 mm and 1.8 mm, respectively at  $V_p = 2.3 - 2.4$  m/s for alumina spheres
- Simulations using a one-step model predicted an ignition temperature 400 K higher than the experimental thresholds
  - Similar trends predicted
  - Use of one-step model not sufficient to capture ignition behavior
  - Have not accounted for surface reactions
  - Have not accounted for species diffusion to the surface
  - Further understanding of the low-temperature oxidation of *n*-hexane needed
- Flame is affected by the presence of the sphere for the mixture composition tested

# Conclusions

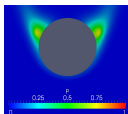
- Simulation predicts ignition to occur in the flow separation region



- The ignition threshold was found to be  $981 \pm 10$  K,  $1010 \pm 25$  K, and  $1159 \pm 10$  K, for sphere diameters of 6.0 mm, 3.5 mm and 1.8 mm, respectively at  $V_p = 2.3 - 2.4$  m/s for alumina spheres
- Simulations using a one-step model predicted an ignition temperature 400 K higher than the experimental thresholds
  - Similar trends predicted
  - Use of one-step model not sufficient to capture ignition behavior
  - Have not accounted for surface reactions
  - Have not accounted for species diffusion to the surface
  - Further understanding of the low-temperature oxidation of *n*-hexane needed
- Flame is affected by the presence of the sphere for the mixture composition tested

# Conclusions

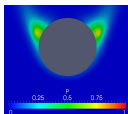
- Simulation predicts ignition to occur in the flow separation region



- The ignition threshold was found to be  $981 \pm 10$  K,  $1010 \pm 25$  K, and  $1159 \pm 10$  K, for sphere diameters of 6.0 mm, 3.5 mm and 1.8 mm, respectively at  $V_p = 2.3 - 2.4$  m/s for alumina spheres
- Simulations using a one-step model predicted an ignition temperature 400 K higher than the experimental thresholds
  - Similar trends predicted
  - Use of one-step model not sufficient to capture ignition behavior
  - Have not accounted for surface reactions
  - Have not accounted for species diffusion to the surface
  - Further understanding of the low-temperature oxidation of *n*-hexane needed
- Flame is affected by the presence of the sphere for the mixture composition tested

# Conclusions

- Simulation predicts ignition to occur in the flow separation region



- The ignition threshold was found to be  $981 \pm 10$  K,  $1010 \pm 25$  K, and  $1159 \pm 10$  K, for sphere diameters of 6.0 mm, 3.5 mm and 1.8 mm, respectively at  $V_p = 2.3 - 2.4$  m/s for alumina spheres
- Simulations using a one-step model predicted an ignition temperature 400 K higher than the experimental thresholds
  - Similar trends predicted
  - Use of one-step model not sufficient to capture ignition behavior
  - Have not accounted for surface reactions
  - Have not accounted for species diffusion to the surface
  - Further understanding of the low-temperature oxidation of *n*-hexane needed
- Flame is affected by the presence of the sphere for the mixture composition tested

# Acknowledgements

The present work was carried out in the Explosion Dynamics Laboratory of the California Institute of Technology, S. A. Coronel was supported by [The Boeing Company](#) through a Strategic Research and Development Relationship Agreement CT-BA-GTA-1 and J. Melguizo-Gavilanes by the [Natural Sciences and Engineering Research Council of Canada](#) (NSERC) Postdoctoral Fellowship Program

# Acknowledgements

The present work was carried out in the Explosion Dynamics Laboratory of the California Institute of Technology, S. A. Coronel was supported by [The Boeing Company](#) through a Strategic Research and Development Relationship Agreement CT-BA-GTA-1 and J. Melguizo-Gavilanes by the [Natural Sciences and Engineering Research Council of Canada](#) (NSERC) Postdoctoral Fellowship Program

# Thank You